

Numerical Investigation into the Effect of Incidence Flow Angles on Submarine Propeller Hydrodynamic Characteristics

H. Kim¹, Z.Q. Leong¹, D. Ranmuthugala^{1,2}, D. Clarke², J. Binns¹ and J. Duffy¹

¹Australian Maritime College,
University of Tasmania, Launceston, Tasmania 7248, Australia

²Defence Science Technology Group
Fishermans Bend, Victoria 3207, Australia

Abstract

This study uses Computational Fluid Dynamics (CFD) to investigate the forces and moments acting on a generic submarine propeller at various inflow angles. The propeller is examined for both the Open Water Condition (OWC) and Behind Hull Condition (BHC). For the latter, a fully appended BB2 generic submarine hull is used as it represents a typical conventional (SSK) submarine.

The results for both the OWC and BHC show that the propeller thrust and torque vary significantly with angles of incidence; with the BHC having the greatest variation. A greater inflow angle produces more noticeable in-plane loads on the propeller, which will cause a moment that acts to reduce the drift angle of the vessel during manoeuvres.

This work contributes to the understanding of the effect of inflow angles on the propulsion properties of submarine propellers and the development of representative body force propellers. Body force propellers are often used in place of rotating propellers for CFD based free running submarine manoeuvring simulations, thus significantly reducing computational cost.

Introduction

A submarine propeller operating at a drift angle is subjected to asymmetric inflow. This causes non-uniformity in the tangential and radial distributions of the flow velocity onto the propeller surface, leading to variations in the propeller thrust and torque distribution. This results in the propeller generating in-plane forces and moments that affect the dynamic response of a submarine during manoeuvres.

In recent decades, Computational Fluid Dynamics (CFD) has been successfully used to study the hydrodynamic characteristics of propellers. Past work [10, 14] has assessed the capability of CFD methodologies for predicting the propulsion performance of propellers in a pure axial flow under an Open Water Condition (OWC), while [2, 16, 17] investigated the effect that the incidence flow angle has on propulsion performance. This work was further expanded to investigate the effect that a hull has on the propulsion performance in pure axial and oblique flows for surface vessels [3, 15]. However, there is limited literature on the effects due to oblique flow passing over fully appended submarine hull forms. In [5], the propulsion properties were examined using a propeller attached to an un-appended underwater vehicle hull in axial and oblique flows. Although [11] used a fully appended BB2 submarine to gain an insight into the flow physics around the propeller, the study was limited to straight ahead conditions and the accuracy of the force predictions was limited by difficulties associated with the near-wall modelled Large Eddy Simulations (LES) in calculating the skin friction on the vehicle. Thus, further work is still required to address the effects of incidence flow on propellers placed behind fully appended submarines.

The aim of this study is to investigate the effects of incidence flow angles on the forces and moments acting on a propeller behind a fully appended submarine. The CFD predictions are first validated against experimental data [13] at various inflow speeds under a zero-angle OWC. The validated simulation model is used to predict the forces and moments acting on a propeller at an angle of incidence to the flow in the horizontal and vertical planes for both the OWC and the Behind Hull Condition (BHC) using a fully appended BB2 generic submarine hull form [7].

Investigation Programme

The present study used a 1:18.35 scale model of the 70m generic submarine geometry and the MARIN 7371R propeller (see Figure 1), which was used in the BB2 submarine free-running tests [9, 12].

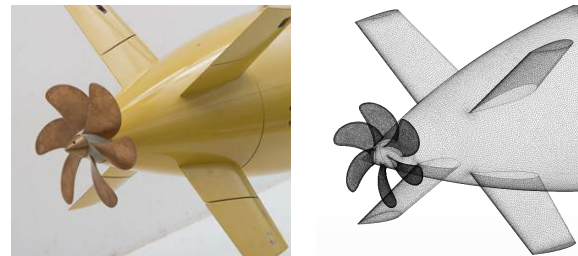


Figure 1. Physical [12] and CFD discretised [9] 6-blade MARIN 7371R stock propeller. The propeller has a diameter of 0.273m with a hub-to-diameter ratio of 0.215:1 and a pitch of 0.263m at 70% of the propeller radius

The forces and moments acting on the propeller were predicted using a 6-DOF body coordinate frame of reference (see Figure 2), in which the positive directions along the x , y and z axes are specified as forward, starboard, and vertically downwards respectively.

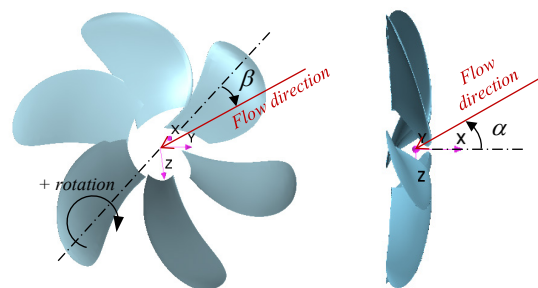


Figure 2. Coordinate system showing horizontal incidence angle (β) and vertical incidence angles (α)

For both the OWC and BHC, the propeller hydrodynamic characteristics are examined at two incidence flow angles (6° and 12°) in the horizontal and vertical planes. The rotating speed of the propeller is set to 266rpm, representative of the

operating speed adopted from the free-running BB2 test [9, 12]. Table 1 summarises the simulation cases considered in the present study. The CFD results were first validated for pure axial inflow against available experimental data [13]. Note that the simulation conditions are limited to non-cavitating flow and deep submersion.

	Flow velocity [m/s]	Horizontal angle (β) [°]	Vertical angle (α) [°]
OWC	0.4 to 1.0	0	0
	1.0	-6, -12, 6, 12	0
	1.0	0	-6, -12, 6, 12
BHC	1.0	0	0
	1.0	-6, -12	0
	1.0	0	-6, -12

Table 1. Simulation cases of the propeller in the Open Water Condition (OWC) and Behind Hull Condition (BHC)

CFD Simulation Setup

The CFD simulations were conducted using Reynolds Averaged Navier–Stokes (RANS) equations with the SST $k-\omega$ turbulence model using the commercial CFD software, Star CCM+ v11.02.10. The boundary conditions applied are as follows: no-slip walls on the propeller and mounting strut/submarine; overset interface on the inner rectangular shape; velocity inlet forward of the propeller/submarine at a specified flow velocity; and a pressure outlet boundary with zero relative pressure at the sides (see Figure 3).

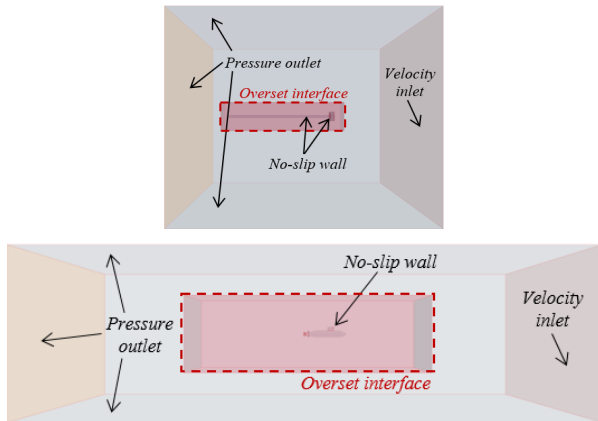


Figure 3. Boundary conditions for (top) Open Water Condition (OWC) and (bottom) Behind Hull Condition (BHC)

All simulations were carried out under transient conditions with a time step of 0.0010s, which corresponds to a 1.6° propeller rotation for each time step. The single-phase fluid is incompressible and isothermic fresh water with density and dynamic viscosity of 997.6kg/m^3 and $8.8871(10^{-4})\text{kg/(m}\cdot\text{s)}$. The simulations employed the high-order advection scheme.

The grid dependence check was carried out under the OWC at a flow velocity of 1.0m/s. Table 2 presents the percentage differences of thrust and torque at each grid level against those at the fine grid. The medium grid was observed to provide acceptable grid-independent predictions and was thus used for the rest of the study.

Grid level	Cells in the propeller cylinder (10^6)	%D of thrust	%D of torque
Coarse	5.01	0.75	2.23
Medium	9.82	0.63	2.00
Fine	19.05	-	-

Table 2. Grid dependence study showing the percentage differences of thrust and torque at each grid level against those at the fine grid

The grid size on the cylindrical interface connecting the propeller and the surrounding fluid flow was prescribed to rotate approximately one grid face per the applied time step (see Figure 4). Additional grid refinement was carried out on the far field regions. The y^+ values were designed to achieve as less than one for the propeller and a minimum of 30 for the hull. Note that the grid sizing on the vehicle surface is set as the medium grid level [9], and details of the grid generation were the same as in [8, 9].

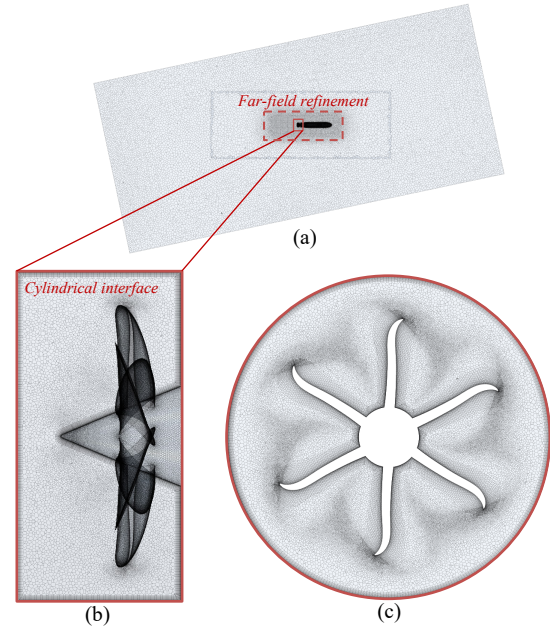


Figure 4 (a) Unstructured hybrid polyhedral grid on $z = 0$ plane for the BHC at 12degrees incidence angles, (b) magnified view of propeller on $y = 0$ plane and (c) $x = 0$ plane

Results and Discussion

The propeller characteristics are analysed in terms of global quantities in the form of non-dimensional parameters (i.e. thrust (K_t) and torque (K_q) coefficients and efficiency (η) along the x , y , and z axes) in accordance with [6]. Note that this study uses the time-averaged values from a complete cycle in which the averaged values did not vary over one rotation.

OWC – Various Inflow Speeds at Zero Incidence Angle

The CFD predictions of thrust and torque were validated against experimental data [13] at the various advance coefficients (J) [6] under the zero-angle OWC. Figure 5 shows K_t , K_q , and η as functions of J . The CFD predictions are found to be in good agreement with the experimental measurements, within a maximum discrepancy of 2.33%, 10.77%, and 7.66% for K_t , K_q , and η , respectively, at the highest J (i.e. 0.83), which was the lightest load applied on the blades in these simulations. The errors are attributed to the CFD computation assumption that the boundary layer on the blades is fully turbulent. As stated in [1], a laminar region exists on the blade suction side in the experiment conducted at model scale. This is further supported in [14], which highlighted that CFD simulations based on laminar flow predicted less torque with nearly unchanged thrust, compared to those in the fully turbulent flow regime. As the torque was over-predicted in the present simulation, the laminar region existing on the blade during the experiment was considered the main source of the difference. Nonetheless, the predictions showed sufficient credibility in the current numerical method and setup; and was thus adopted for the remaining simulation cases in the study.

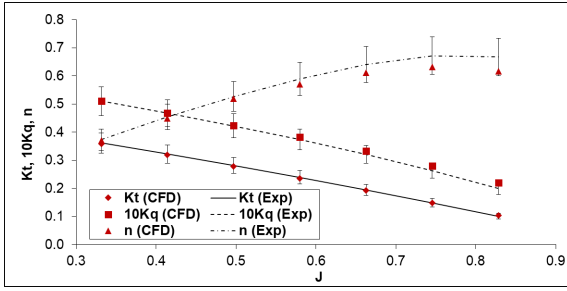


Figure 5. Thrust and torque coefficients of MARIN 7371R propeller at various advance coefficient (J) in the OWC [13]. Error bars of 10% have been included for illustrative purposes.

OWC - Various Incidence Flow Angles in Horizontal and Vertical Planes

The effect of incidence flow angles on thrust and torque were investigated under the OWC at an inflow speed of 1m/s. Figure 6 shows the prediction of the thrust forces along the x , y , and z axes at two incidence flow angles (6° and 12°). In both the horizontal and vertical planes, it was observed that the asymmetric inflow at the propeller creates stronger forces in all directions, in comparison to the symmetric inflow condition at the zero-incidence angle. The magnitude of the thrust and torque were found to be identical in the $+$ and $-$ incidence angles. Focusing on the individual load components, it is seen that in-plane thrust components, Kty and Ktz , have a linear relationship with the incidence angle, whereas Ktx shows a gradual increase with increasing incidence angle.

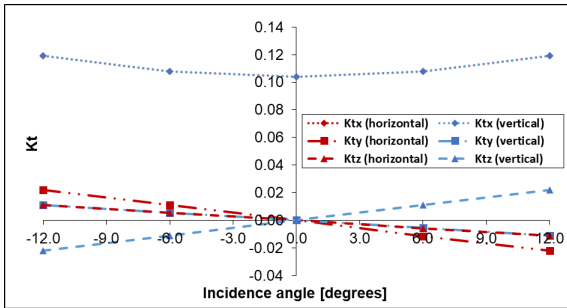


Figure 6. Thrust coefficients in x , y and z axes in horizontal and vertical planes

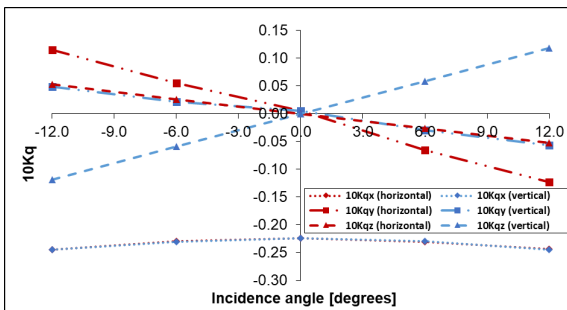


Figure 7. Torque coefficients in x , y and z axes in horizontal and vertical planes

The increase in the forces along all axes leads to the requirement for more power, leading to a rise in the torque at the same level of increase as the forces. Figure 7 shows that Kqx , Kqy , and Kqz follow the same distribution law as Ktx , Kty , and Ktz . It is seen that in-plane torque components, Kqy and Kqz , become significant at higher angles, showing an increase in the asymmetric loadings on the blades with respect to the x - z and x - y planes.

BHC - various incidence angles of flow in horizontal and vertical planes

In comparison to the zero-angle OWC at the same free stream axial velocity (V), the thrust and torque under the BHC are greater owing to the wake induced in the stern region of the submarine. The wake leads to a reduction in an inflow velocity (V_A) and producing more thrust. Table 3 indicates that the wake velocity expressed in the form of the Taylor wake fraction factor (w_T) [6] is highest at zero angle and decreases slightly with an incidence flow in the horizontal and vertical planes. Overall, up to -12° , it is seen that the flow angle has a minimal effect in the axial wake velocity. Note that V_A is obtained by averaging the velocity on a plane with a diameter of $1.1D$ [9] placed $0.2D$ forward from the propeller origin (Figure 2).

Incidence angles	V [m/s]	V_A [m/s]	w_T
0	1	0.73	0.27
-6 (horizontal)	1	0.75	0.25
-12 (horizontal)	1	0.76	0.24
-6 (vertical)	1	0.76	0.24
-12 (vertical)	1	0.76	0.24

Table 3. Taylor wake fraction factor (w_T) at different angles of incidence at prescribed free stream axial velocity (V) and advance velocity (V_A) to the propeller

The behind-hull performance of the propeller at different flow angles was investigated in terms of the forces along the x , y , and z axes (see Figure 8). It is observed that greater negative flow angles in the horizontal plane resulted in higher axial forces compared to that at the zero-incidence angle. The higher axial forces are mainly attributable to the direction of the in-plane tangential velocity that is directed opposite to the propeller rotation direction. The opposite direction to the propeller rotation causes an increase in the blade angles of attack and thus increasing the axial forces [15]. However, greater negative angles in the vertical plane resulted in lower axial forces owing to that the direction of the in-plane tangential velocity is consistent with the propeller rotation direction.

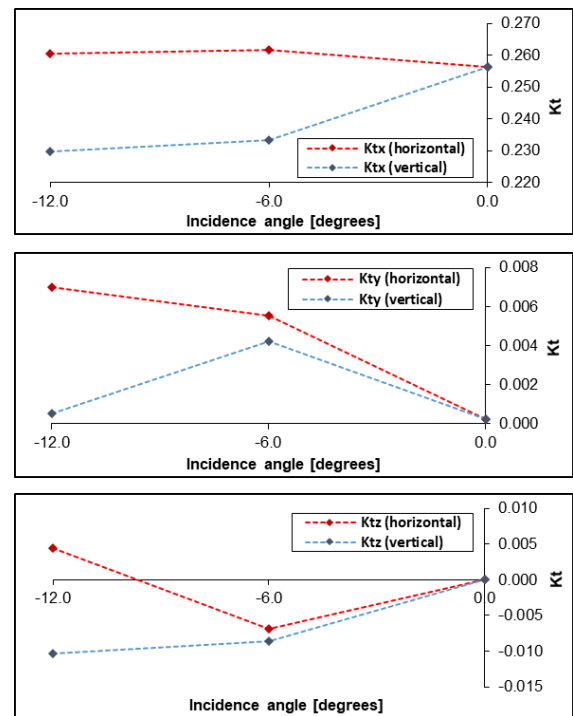


Figure 8. Thrust and torque coefficients in x (top), y (middle) and z (bottom) axes in horizontal and vertical planes for the Behind Hull Condition (BHC)

The side force in the horizontal plane and the vertical force in the vertical plane increased with the flow angle, as expected. It is seen that compared to the OWC the greater force variations in all axes are occurred under the BHC owing to the presence of a hull-generated wake that adds non-uniformity into the flow in front of the propeller (see Figure 9).

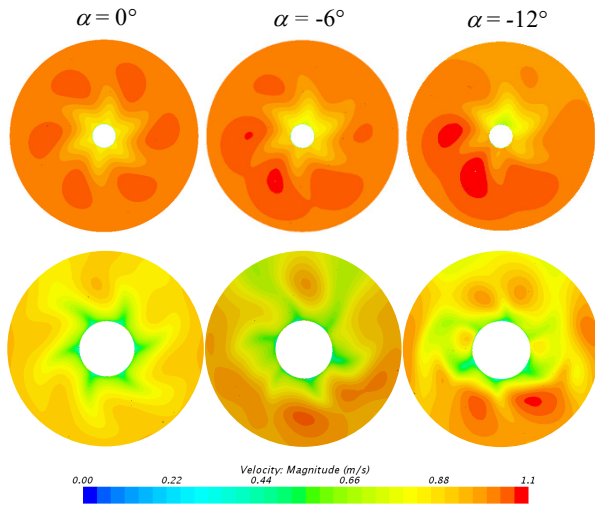


Figure 9. Instantaneous velocity distribution on a plane at $x = 0.1D$ under the (top) Open Water Condition (OWC) and (bottom) Behind Hull Condition (BHC) at vertical incidence angles 0° , -6° and -12° at $V = 1\text{m/s}$

Conclusions

This paper presents an investigation into the effect that the inflow angles have on the hydrodynamic characteristics of a submarine propeller in terms of the global load components (axial load and in-plane loads incorporating side and vertical loads). The variations in the loads are examined at two inflow angles (i.e. 6° and 12°) in the horizontal and vertical planes for both the OWC and BHC.

The results show that an increase in the inflow angle generates more in-plane loads on the propeller as well as an axial load; with the greatest variations in the loads occurring in the BHC. The visualisation of the asymmetrical load on the propeller supported the comprehension of force variations with the inflow angle. The present work contributes to understanding the effect that the inflow angle has on the propulsion properties of submarine propellers. This is imperative in order to improve the hydrodynamic design and matching of propellers and formulating effective control strategies of the vehicle [4].

Further work is being undertaken to investigate the fluctuating blade loads in time domain as they could cause vibration during operation. The results are intended to be utilised to improve the body force propeller capability in 6-DOF CFD submarine manoeuvring simulations to address the limitations in representing the actual propeller when operating at a drift angle [9].

Acknowledgments

The authors would like to thank the Defence Science and Technology (DST) Group for the financial and technical support during the project.

References

[1] Carlton, J. (2012). *Marine propellers and propulsion*. Butterworth-Heinemann.

[2] Dubbioso, G., Muscari, R., & Di Mascio, A. (2013). Analysis of the performances of a marine propeller operating in oblique flow. *Computers & Fluids*, 75, 86-102.

[3] Dubbioso, G., Muscari, R., Ortolani, F., & Di Mascio, A. (2017). Analysis of propeller bearing loads by CFD. Part I: straight ahead and steady turning maneuvers. *Ocean Engineering*, 130, 241-259.

[4] Geertsma, R. D., Negenborn, R. R., Visser, K., & Hopman, J. J. (2017). Design and control of hybrid power and propulsion systems for smart ships: A review of developments. *Applied Energy*, 194, 30-54.

[5] Hayati, A. N., Hashemi, S. M., & Shams, M. (2013). A study on the behind-hull performance of marine propellers astern autonomous underwater vehicles at diverse angles of attack. *Ocean Engineering*, 59, 152-163.

[6] ITTC. (2014). ITTC Symbols and Terminology List. In *Proceedings of the 27th Int Towing Tank Conference*.

[7] Joubert, P. N. (2006). Some aspects of submarine design. Part 2. Shape of a submarine 2026 (No. DSTO-TR-1920). Defence science and technology Group.

[8] Kim, H., Leong, Z. Q., Ranmuthugala, D., & Forrest, A. (2015). Simulation and Validation of an AUV in Variable Accelerations. *International Journal of Offshore and Polar Engineering*, 25(01), 35-44.

[9] Kim, H., Ranmuthugala, D., Leong, Z. Q., & Chin, C. (2018). Six-DOF simulations of an underwater vehicle undergoing straight line and steady turning manoeuvres. *Ocean Engineering*, 150, 102-112.

[10] Morgut, M., & Nobile, E. (2012). Influence of grid type and turbulence model on the numerical prediction of the flow around marine propellers working in uniform inflow. *Ocean Engineering*, 42, 26-34.

[11] Norrison, D., Sidebottom, W., & Anderson, B. (2016). Numerical Study of a Self-Propelled Conventional Submarine. In *31st Symposium on Naval Hydrodynamics*.

[12] Overpelt, B., Nienhuis, B., & Anderson, B. (2015). Free Running Manoeuvring Model Tests On A Modern Generic SSK Class Submarine (BB2). In *Proceedings of PACIFIC 2015 Int. Maritime Conf., Sydney, NSW, Australia*.

[13] Pontarelli, M., Martin, J. E., & Carrica, P. M. (2017). Dynamic Instabilities in Propeller Crashback. In *Proceedings of 5th International Symposium on Marine Propulsors*.

[14] Rhee, S. H., & Joshi, S. (2005). Computational validation for flow around a marine propeller using unstructured mesh based Navier-Stokes solver. *JSME International Journal Series B Fluids and Thermal Engineering*, 48(3), 562-570.

[15] Sun, S., Li, L., Wang, C., & Zhang, H. (2018). Numerical prediction analysis of propeller exciting force for hull-propeller-rudder system in oblique flow. *International Journal of Naval Architecture and Ocean Engineering*, 10(1), 69-84.

[16] Wang, C., Sun, S., Sun, S., & Li, L. (2017). Numerical analysis of propeller exciting force in oblique flow. *Journal of Marine Science and Technology*, 22(4), 602-619.

[17] Yao, J. (2015). Investigation on hydrodynamic performance of a marine propeller in oblique flow by RANS computations. *International Journal of Naval Architecture and Ocean Engineering*, 7(1), 56-69.